International Dairy Journal 99 (2019) 104538

Contents lists available at ScienceDirect

International Dairy Journal

journal homepage: www.elsevier.com/locate/idairyj

Increasing calcium solubility from whey mineral residues by combining gluconate and δ-gluconolactone

Andressa de Zawadzki, Leif H. Skibsted*

Department of Food Science, University of Copenhagen, Rolighedsvej 26, DK-1958, Frederiksberg C, Denmark

ARTICLE INFO

Article history:
Received 25 February 2019
Received in revised form
17 July 2019
Accepted 21 July 2019
Available online 7 August 2019

ABSTRACT

Insoluble milk mineral residues from whey processing, dominated by hydroxyapatite and calcium hydrogen phosphate, dissolved isothermally in aqueous gluconate/δ-gluconolactone, spontaneously forming solutions supersaturated in both calcium hydrogen phosphate and calcium gluconate. Calcium concentration of maximally supersaturated solutions was proportional to gluconate concentration, indicating gluconate assisted dissolution, while gluconolactone increased calcium available for dissolution and supersaturation. Precipitation of calcium gluconate, rather than of calcium hydrogen phosphate, was critical for supersaturation robustness. For calcium gluconate ionic product:solubility product of calcium gluconate ratios <12, the supersaturated solutions had a lag phase for precipitation of several weeks, which increased to several months by addition of solid calcium saccharate prior to dissolution of the mineral residues. Such supersaturated solutions with up to 7 g calcium L^{-1}, corresponding to a factor of supersaturation of >100 times compared with equilibrium calcium hydrogen phosphate solubility, may be exploited for increasing calcium availability of whey mineral based functional foods.

1. Introduction

Side-streams from cheese production may lead to other valuable dairy products based on whey proteins and lactose (Harju, 2001; Prazeres, Carvalho, & Rivas, 2012; Sizo, 1996). Part of the milk minerals are, however, still left dissolved in the whey permeate in an amount depending on the actual cheese produced (Gaucheron, 2005, 2011; Kelly & O'Kennedy, 2001). The minerals, including the essential calcium and magnesium together with phosphate, may be collected as a powder by evaporation rather than becoming a polluting waste (Gaucheron, 2005). Such powders have, moreover, an optimal calcium/phosphate ratio for human nutrition and increasingly find use as ingredients in various food products and as part of food supplements. A low bioavailability of especially calcium from such preparations, however, often becomes a problem for their optimal use (Kato et al., 2002; Lorieau et al., 2018; Prazeres et al., 2012). Calcium is mainly present in such powders after drying as amorphous calcium hydrogen phosphate and hydroxyapatite, both of which calcium phosphate salts have low aqueous solubility and, moreover, a slow dissolution rate in acid (Wu & Uskoković, 2016).

Calcium hydroxycarboxylates, such as calcium gluconate and calcium citrate, are often used in food supplements for prevention of osteoporosis (Straub, 2007; Sunyecz, 2008). Sodium gluconate and sodium citrate have, together with other hydroxycarboxylates, recently been shown to dissolve sparingly soluble calcium phosphates, spontaneously forming strongly supersaturated aqueous solutions (Cheng & Skibsted, 2018; Vavrusova, Danielsen, Garcia, & Skibsted, 2018; Vavrusova, Garcia, Danielsen, & Skibsted, 2017; Vavrusova & Skibsted, 2014). Such supersaturation seems to prevent precipitation of calcium salts of low solubility in the intestines and may explain the high bioavailability of calcium from calcium hydroxycarboxylates compared with other calcium salts such as calcium carbonate, which dissolve in the acid of the stomach but subsequently precipitate in the intestines (Skibsted, 2016).

Calcium from whey mineral residues needs to dissolve during food digestion to become available for absorption in the intestines. Gluconate seems in combination with gluconic acid to hold the potential of solubilising whey mineral residues, forming moderately acidic but highly robust supersaturated solutions with the milk calcium phosphates (Cheng & Skibsted, 2018). Accordingly, we have investigated dissolution and tendency of precipitation of a commercial whey mineral product in aqueous gluconate/gluconolactone with special focus on the robustness of the supersaturation relative to precipitation.

* Corresponding author. Tel.: +45 3533 3221.
E-mail address: ls@food.ku.dk (L.H. Skibsted).

https://doi.org/10.1016/j.idairyj.2019.104538
0958-6946/

2. Materials and methods

2.1. Materials

Capolac® MM-0525 BG was a commercial dried milk mineral concentrate from Arla Food Ingredients (Viby J., Denmark) based on whey from bovine cheese production. According to product specifications it contains 24.0–29.0% calcium, 11.0–15.0% phosphorous, 6.0–10.0% lactose, less than 3.0% moisture, less than 3.0% protein and less than 3.0% fat. All investigations used material from the same batch, which was analysed by inductively coupled plasma (ICP) spectroscopy (see below) and found to contain 26.5% calcium and 13.3% phosphorous.

Sodium hydrogen citrate sesquihydrate, D-gluconic acid sodium salt (≥99%), D-gluconic acid δ-lactone, calcium saccharate, calcium standard for ICP spectroscopy (10,005 ± 20 mg L^{-1}), phosphorous standard for ICP spectroscopy (9992 ± 20 mg L^{-1}), nitric acid 65% Suprapur®, were all from Sigma-Aldrich (Steinheim, Germany). Calcium chloride dihydrate was from Merck KGaA (Darmstadt, Germany); 0.01 D KCl (±0.5%, 25 °C) as a conductivity standard was from HACH LANGE GmbH (Berlin, Germany). Q-Max RR syringe filters (filter diameter: 13 mm, membrane: 0.22 μm cellulose acetate) were from Frisenette ApS (Knebel, Denmark). All solutions were prepared using purified water from a Milli-Q Plus purification station (Millipore Corporation, Bedford, MA, USA).

2.2. Dissolution of Capolac®, δ-gluconolactone and sodium gluconate

Mixtures containing samples of Capolac®, D-gluconic acid sodium salt (gluconate) and D-gluconic acid δ-lactone (gluconolactone) were prepared to identify the most suitable combinations for dissolution of calcium phosphate salts present in Capolac®. One hundred millilitres of Milli Q water were added to flasks containing 1.40 g Capolac®. The mixtures were equilibrated for 1 day at 25 °C with stirring, then (A) 12.6 g sodium gluconate and 5.2 g gluconolactone (combination gluconate/gluconolactone 2:1 = 5.8×10^{-2} mol/2.9×10^{-2} mol); (B) 6.9 g of sodium gluconate and 5.6 g gluconolactone (combination gluconate/gluconolactone 1:1 = 3.2×10^{-2} mol/3.2×10^{-2} mol); (C) 3.6 sodium gluconate and 5.9 g gluconolactone (combination gluconate/gluconolactone 1:2 = 1.7×10^{-2} mol/3.3×10^{-2} mol). Also, for the combination 6.9 g sodium gluconate and 5.6 g gluconolactone (gluconate/gluconolactone 1:1) a suspension was prepared with 1×10^{-3} mol solid calcium saccharate added. Turbidity, calcium ion activity and pH were measured over 8 days to follow the formation and robustness of supersaturated solutions of calcium salts from Capolac®. After each equilibration period, aliquots were collected and filtered for measurement. Calcium concentration and phosphorus concentration were determined by inductively coupled plasma atomic emission spectroscopy (ICP-AES).

2.3. Electrochemical determination of free calcium

A calcium ion selective electrode ISE25Ca with a reference REF251 electrode from Radiometer (Copenhagen, Denmark) was used to determine calcium ion activity. Calcium chloride standard solutions (1.00×10^{-4}, 1.00×10^{-3} and 1.00×10^{-2} mol L^{-1}, prepared from a 1.00 mol L^{-1} stock solution) were used to calibrate the electrode. A linear standard curve of the potential (mV) against the corresponding −log (aCa^{2+}) was established in agreement with the Nernst equation using linear regression. The slope of the regression curve was found in agreement with the Nernst equation. Calcium ion activity $a_{Ca^{2+}}$ for the standard curve was calculated according to:

$$a_{Ca^{2+}} = c_{Ca^{2+}} \times \gamma^{2+} \quad (1)$$

where γ^{2+} is the activity coefficient based on the Davies' equation as previously described (Vavrusova et al., 2018):

$$\log \gamma^{2+} = -A_{DH} z^2 \left(\frac{\sqrt{I}}{1+\sqrt{I}} - 0.30I \right) \quad (2)$$

where A_{DH} is the Deybe-Hückel constant with a value of 0.500, 0.506, 0.510, 0.515 at 15, 20, 25 and 30 °C, respectively. The ionic strength is defined as:

$$I = \frac{1}{2} \sum_i c_i z_i^2 \quad (3)$$

where c_i is the concentration of the ions in the solution, and z_i is the corresponding charge.

2.4. Ion coupled plasma optical emission spectroscopy (ICP-OES)

Aliquots of the solutions containing Capolac® and gluconate/gluconolactone were collected from the soluble fraction (permeate) and filtered in syringe filters (pore size 0.22 μm). Ten microlitres of the samples were diluted to 10 mL in 5% HNO_3, and subsequently analysed by ICP spectroscopy. The standard samples with the concentration of 10.005, 5.003, 2.501, 1.251 and 0.625 ppm were prepared from the calcium standard for ICP spectroscopy to make a calibration curve. For phosphorus, standard solutions with the concentration of 0.323, 0.161, 0.0807, 0.0403 and 0.0202 ppm were prepared from the phosphorous standard for ICP spectroscopy to make a calibration curve. Total calcium of the test samples was analysed by coupled plasma-optical emission spectroscopy with an Agilent 5100 ICP-OES (Santa Clara, CA, USA). Multiple-wavelengths (393.366, 396.847 and 422.673 nm) were used to determine the total calcium in the samples. The wavelength of 177.343 nm was used to determine total phosphorous concentration in the samples. Magnesium was also measured by ICP spectroscopy, but the data are not shown because magnesium concentration was found to be constant for all the systems during the whole period of investigation of equilibration.

2.5. pH measurement

A pH metre (713 pH Metre, Metrohm, Herisau, Switzerland) with a glass electrode (602 Combined Metrosensor glass electrode, Metrohm) using international pH activity standards (pH 4.00, 7.00 and 9.00) was used for the measurement of the pH of the solutions containing Capolac® and gluconate/gluconolactone during equilibration.

2.6. Turbidimetry

Turbidity measurements were performed with TurbiDirect AL450T-IR turbidity metre (Aqualytic, Dortmund, Germany) with an incident light (860 nm) through a 25 mm cell at room temperature.

2.7. X-ray diffraction of Capolac®, hydroxyapatite and $CaHPO_4.2H_2O$

X-ray diffraction (XRD) patterns were obtained for Capolac® using a Bruker D8 Advance (Cu Kα 1.5418 Å), which is located at São Carlos Chemistry Institute, University of São Paulo (São Carlos-SP, Brazil). The sample was supported by a silica microslide substrate (1×1 cm^2) and XRD patterns were collected in the range X–Y 2θ degrees. XDR patterns for hydroxyapatite and $CaHPO_4.2H_2O$ were obtained from the database JCPDS X-ray card data collection (2014).

2.8. Calculation of ion speciation

Ion speciation was determined taking into account six equilibrium equations together with three mass balance equations, using the approach previously described (Cheng & Skibsted, 2018). The equilibrium constants for dissociation of phosphoric acid $K_{a1_{H_3PO_4}}$, $K_{a2_{H_3PO_4}}$ and $K_{a3_{H_3PO_4}}$; dissociation of gluconic acid K_{g1}; formation of the $CaHPO_4$ complex, K_1; formation of the $CaH_2PO_4^+$ complex, K_2; and for formation of the $CaGlu^+$ complex, K_3, based on activity were corrected with the respective activity coefficients to constants based on concentration at the actual ionic strength of the solution. Total concentration of calcium and phosphate was determined by ICP spectroscopy. Total gluconate was obtained as the sum of the total molar concentration of δ-gluconolactone and sodium gluconate added to the solutions for the homogeneous supersaturated solutions. Calculations of ion speciation were undertaken by iterations according to Fig. 1. Considering an initial ionic strength of 1.0 mol L^{-1} for the first cycle of calculations, the activity coefficients were determined using Davies equation (Eq. (2)). New values of activity coefficient were calculated with the new value of ionic

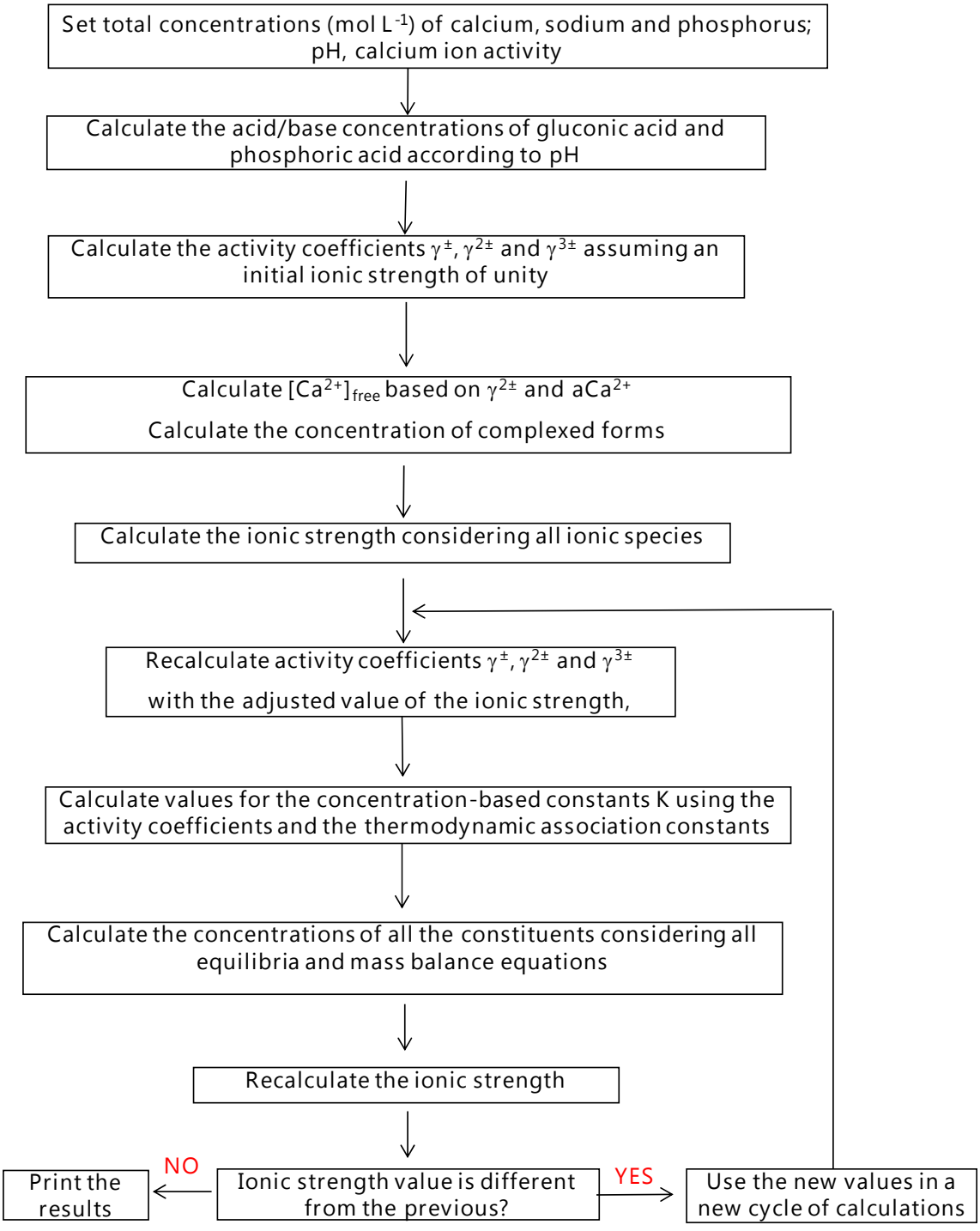

Fig. 1. Method for calculating ion speciation.

strength emerging from the initial calculations and then, the calculation of the ion speciation was repeated with adjusted concentration based equilibrium constants. Iterations were repeated as previously described (Garcia, Vavrusova, & Skibsted, 2018) to obtain a constant value for ionic strength for the actual equilibration time as a criterion for ending the iteration. The final value for ionic strength at the first equilibration time was subsequently replacing the starting value for ionic strength and iteration for the next sampling time.

3. Results and discussion

3.1. Aqueous solubility of Capolac®

The Capolac® sample was found to contain 26.5% calcium and 13.3% phosphorous corresponding to a calcium/phosphate ratio of 1.5, which is close to the calcium/phosphate recommendation for human consumption (Bronner, 2009). The ratio obtained for Capolac® can be accounted for as a mixture of 30% calcium hydrogen phosphate ($CaHPO_4$ with a ratio of 1.0) and 70% hydroxyapatite [$Ca_5(OH)\ (PO_4)_3$ with a ratio of 1.7; Koutsopoulos, 2002]. Although other calcium phosphates may also be present, X-ray powder diffractograms confirmed hydroxyapatite as an important component as may be seen from Fig. 2. The X-ray diffractogram of Capolac® shows a similar X-ray pattern as hydroxyapatite with characteristic broad diffraction peaks at $2\theta = 26°$ and 30–35° (Koutsopoulos, 2002; Venkateswarlu, Chandra Bose, & Rameshbabu, 2010). The broad peaks with low separation are due to a low crystallinity and the powder was found to be largely amorphous, containing amorphous calcium phosphates together with crystalline fractions of compounds like $CaHPO_4.2H_2O$, the peaks for which seem present with lower intensity in the X-ray diffractogram of Capolac®, see Fig. 2.

The aqueous solubility of calcium for Capolac® was determined electrochemically at 10 °C, 25 °C and 50 °C to estimate the enthalpy of dissolution of calcium salts present in Capolac® and to be compared with the heat of dissolution of calcium hydrogen phosphate dihydrate. The calcium ion activity of an aqueous suspension of Capolac® was found to decrease with temperature as measured electrochemically, see Fig. 3. The solubility of the calcium salts in Capolac® corresponds to $a_{Ca^{2+}} = 0.00034$ at 25 °C with $\Delta H = -5.8 \pm 0.7$ kJ mol^{-1} for the overall dissolution process as calculated from the van't Hoff plot of Fig. 3. The heat of dissolution of calcium from Capolac® was found comparable with the heat of dissolution of calcium hydrogen phosphate:

$$CaHPO_4.2H_2O_{(s)} \rightleftharpoons Ca^{2+} + HPO_4^{2-} + 2H_2O \quad (4)$$

for which $a_{Ca^{2+}} = 0.00017$ at 25 °C and $\Delta H = -4.6 \pm 1.0$ kJ mol^{-1} were determined by the same method. The dissolution of $CaHPO_4.2H_2O$ is exothermic and the solubility decreases with increasing temperature like for calcium from Capolac® (McDowell, Sutter, & Brown, 1971). The apparent higher solubility of calcium salts from Capolac® than of $CaHPO_4.2H_2O$ and especially of $Ca_5(OH)\ (PO_4)_3$ confirms the presence of traces of complexing agents in Capolac®. The less negative enthalpy of dissolution of calcium from Capolac® compared with $CaHPO_4.2H_2O$ may be explained by endothermic dissolution of non-ionic species in Capolac®. Capolac® mainly contains calcium hydrogen phosphate, hydroxyapatite and other salts highly insoluble in water (Pan & Darvell, 2010). Other compounds present including lactose and hydroxycarboxylates like citrate may contribute to increase the solubility of calcium from Capolac® and may also affect the supersaturation processes.

3.2. Supersaturation of calcium phosphates from Capolac®

The dissolution of calcium ions from Capolac® was found to increase dramatically by the presence of gluconate and gluconolactone as also previously found for calcium hydrogen phosphate (Cheng & Skibsted, 2018). The increase depends both on the total gluconate concentration and on the ratio between gluconate and gluconolactone as the combination of binding of calcium to gluconate, Glu^-:

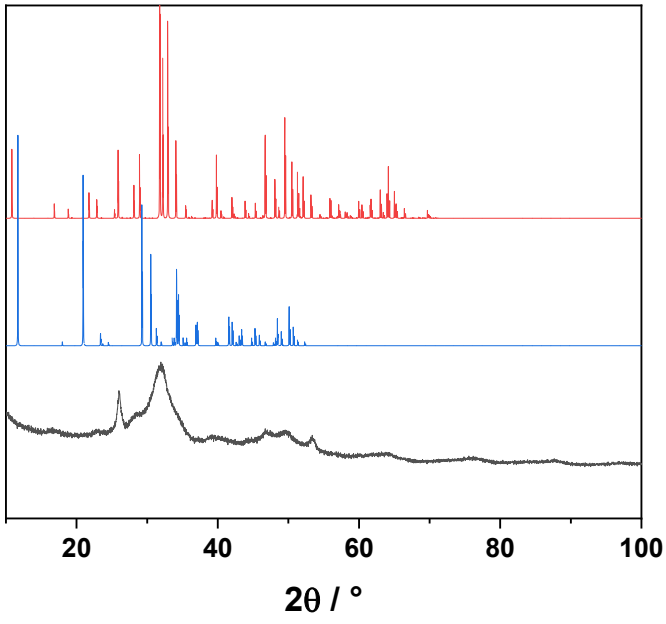

Fig. 2. X-ray powder diffraction (XDR) of Capolac® (——) in comparison with $CaHPO_4.2H_2O$ (——) and hydroxyapatite (——). (For interpretation of the references to color in this figure legend, the reader is referred to the Web version of this article.)

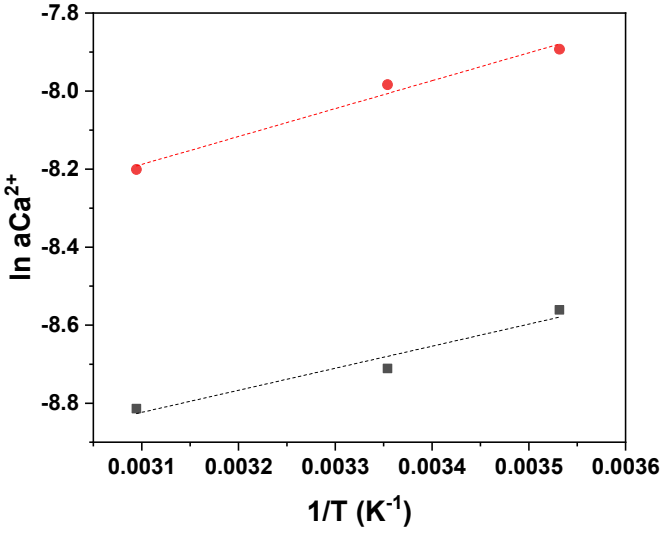

Fig. 3. Calcium ion activity of water saturated with Capolac® (●) as measured electrochemically or saturated with $CaHPO_4.2H_2O$ (■). The enthalpy of dissolution was calculated from the temperature dependence according to $ln(aCa^{2+}) = \frac{-\Delta H^0}{RT} + constant$, by linear regression to yield $\Delta H = -5.8 \pm 0.7$ kJ mol^{-1} K^{-1} for Capolac® and $\Delta H = -4.6 \pm 0.6$ kJ mol^{-1} K^{-1} for $CaHPO_4.2H_2O$. (For interpretation of the references to color in this figure legend, the reader is referred to the Web version of this article.)

$$Ca^{2+} + Glu^{-} \rightleftharpoons CaGlu^{+} \quad (5)$$

and dissolution due to protonation of phosphate and hydrogen phosphate by the more acidic gluconic acid, HGlu, both become important:

$$Ca_5(PO_4)_3OH + 4HGlu \rightleftharpoons 3CaHPO_4 + 2CaGlu^{+} + 2Glu^{-} + 2H_2O \quad (6)$$

$$CaHPO_{4(s)} + HGlu \rightleftharpoons CaGlu^{+} + H_2PO_4^{-} \quad (7)$$

The dissolution was moreover seen to overshoot the equilibrium solubility of the calcium salts from Capolac® as was evident from a subsequent precipitation following a lag phase with a length depending on the degree of supersaturation. A more detailed analysis was made for four dissolution conditions. In each experiment, 1.4 g of Capolac® was suspended in 100 mL of water with sodium gluconate and gluconolactone added. For the four selected conditions clear solutions appeared within a few hours. For the dissolution experiment with calcium saccharate added, dissolution was, however, somewhat slower. Each of these solutions was analysed for total calcium and total phosphate by ICP spectroscopy, and pH and calcium ion activity were measured together with turbidity during subsequent incubation at 25 °C for one week, and for the dissolution with saccharate the calcium ion activity was measured for one month.

The development in calcium activity, calcium concentration and pH is shown in Figs. 4 and 5. pH was for all four solutions decreasing due to hydrolysis of gluconolactone and calcium concentration increased to reach maximal values after approximately 2 h. For each of the three experiments without calcium saccharate, the ionic speciation based on iterative calculations are presented in Table 1 (gluconate/gluconolactone = 2:1), Table 2 (gluconate/gluconolactone = 1:1) and Table 3 (gluconate/gluconolactone = 1:2). Notably, free calcium concentration increased for decreasing pH during incubation and became highest for the supersaturation solution with lowest final pH. This increase in free calcium ion concentration is understood on the basis of decreasing concentration of free gluconate and hydrogen phosphate with decreasing pH due to protonation leaving less calcium coordinated. The final pH of the three solutions, pH = 4.1 for gluconate/gluconolactone = 2:1, pH = 3.8 for gluconate/gluconolactone = 1:1, pH = 3.6 for gluconate/gluconolactone = 1:2, is in agreement with

$$pH = pK_a + \log\frac{[Glu^{-}]}{[HGlu]} \quad (8)$$

and a pKa ≅ 3.8 for gluconic acid at an ionic strength around 0.5 (Skibsted & Kilde, 1971).

For the experiment presented in Table 1 with a total gluconate concentration of 87 mmol 100 mL^{-1} with gluconate/gluconolactone ratio of 2:1, precipitation was initiated after 6 days of incubation of this solution, as also is evident from the turbidity measurements (Fig. 6). Addition of solid calcium hydrogen phosphate to samples of this 2:1 gluconate/gluconolactone solution during early incubation where the solution was fully transparent did not initiate turbidity and precipitation, while addition of solid calcium gluconate initiated precipitation. Based on these observations, it was concluded that the precipitate spontaneously formed after 6 days of incubation was calcium gluconate rather than calcium hydrogen phosphate:

$$Ca^{2+} + 2Glu^{-} \rightleftharpoons CaGlu_{2(s)} \quad (9)$$

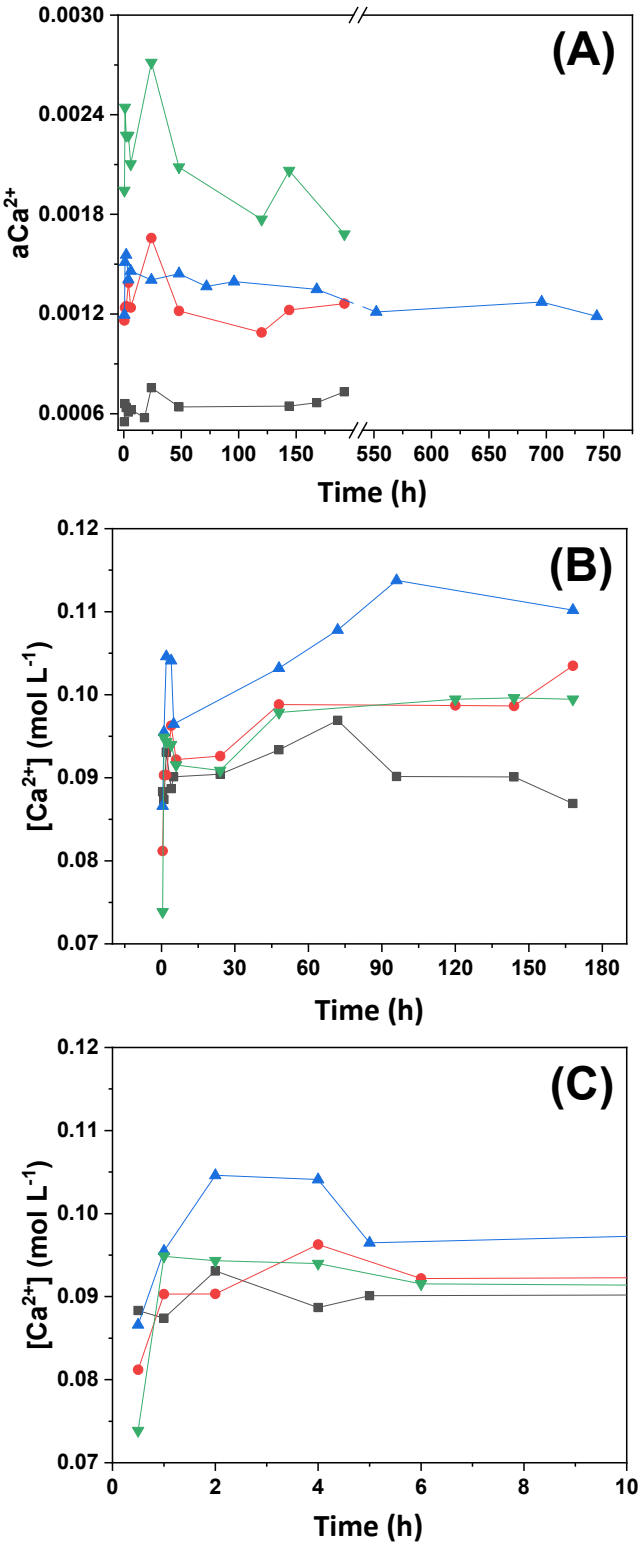

Fig. 4. Calcium ion activity (A) and total calcium concentration (B) of homogeneous solutions containing 1.4 g of Capolac® in 100 mL of water dissolved in aqueous combinations of gluconate/gluconolactone 2:1 = 5.8×10^{-2} mol/2.9×10^{-2} mol (■), gluconate/gluconolactone 1:1 = 3.2×10^{-2} mol/3.2×10^{-2} mol (●), gluconate/gluconolactone 1:1 = 3.2×10^{-2} mol/3.2×10^{-2} mol plus 1×10^{-3} mol of calcium saccharate (▲); gluconate/gluconolactone 1:2 = 1.7×10^{-2} mol/3.4×10^{-2} mol (▼). aCa^{2+} and $[Ca^{2+}]$ were measured after 30 min and during 8 days of incubation at 25 °C. (C) Details of the initial concentration of calcium for all combinations. (For interpretation of the references to color in this figure legend, the reader is referred to the Web version of this article.)

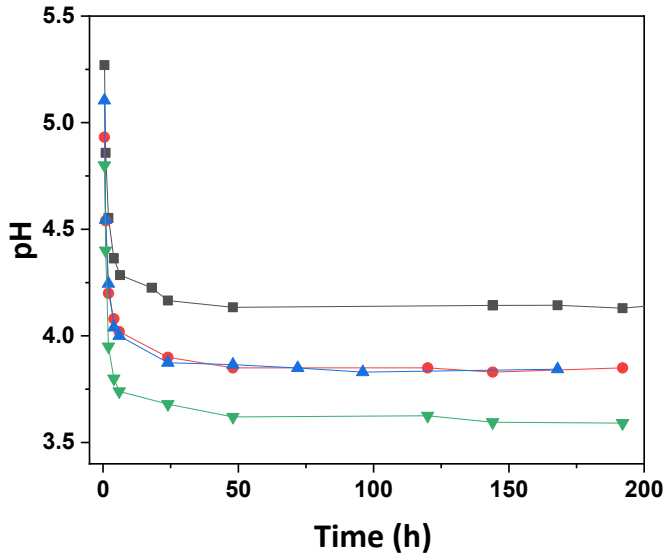

Fig. 5. pH variation of aqueous solutions or suspensions containing 1.4 g of Capolac® in 100 mL of water for gluconate/gluconolactone with a ratio of 2:1 (■), gluconate/gluconolactone 1:1 (●), gluconate/gluconolactone with a ratio of 1:1 and 1×10^{-3} mol of calcium saccharate (▲) and gluconate/gluconolactone with a ratio of 1:2 (▼). pH was measured after 30 min and during 8 days of incubation at 25 °C. (For interpretation of the references to color in this figure legend, the reader is referred to the Web version of this article.)

The phosphate concentration was not affected by the precipitation further confirming this conclusion.

For the experiment presented in Table 2, a total gluconate concentration of 64 mmol was used with gluconate/gluconolactone ratio of 1:1. This solution showed no precipitation until after 2 weeks, which also was true for the experiment of Table 3 with a total of 50 mmol of gluconate and a gluconate/gluconolactone ratio of 1:2. The experiment of Table 3 with 64 mmol of total gluconate was repeated with the addition of 1×10^{-3} mol of solid calcium saccharate to the transparent solution together with solid Capolac®. Calcium saccharate dissolved slowly as was evident from an initial turbidity disappearing concomitant with an increase in calcium concentration. The total calcium concentration and the calcium ion activity as followed over 180 h are shown in Fig. 4.

For the solutions without precipitation, the total calcium ion concentration stayed constant as to be expected, while for the solution with precipitation, the total calcium concentration decreased. For the solution with calcium saccharate added, the total calcium concentration slowly increased, as calcium saccharate (CaSac) was slowly dissolved through a stepwise process in which the complex will only partially dissociate ($K_a = 1.0 \times 10^3$, $K_{sp} = 6.17 \times 10^{-7}$ at 25 °C):

$$CaSac_{(s)} \rightleftharpoons CaSac_{(aq)} \quad (10)$$

$$CaSac_{(aq)} \rightleftharpoons Ca^{2+} + Sac^{2-} \quad (11)$$

Calcium activity of suspensions containing Capolac® and the three different combinations of gluconate/gluconolactone showed no significant changes for up to 8 days of incubation under magnetic stirring at 25 °C (Fig. 4A). However, calcium ion activities were found to decrease with increasing concentrations of gluconate as expected since the complex formation of calcium gluconate increases with higher concentrations of gluconate as ligand. The concentration of gluconolactone relative to gluconate also

Table 1
Ion speciation in supersaturated homogeneous solution at 25 °C resulting from dissolution of 1.4 g of Capolac®, 5.8×10^{-1} mol L^{-1} of gluconate and 2.9×10^{-1} mol L^{-1} of δ-gluconolactone in water (100 mL).[a]

Time (h)	pH	aCa^{2+}	$[Ca^{2+}]_T$	[P]	$[CaHPO_4]$	$[CaH_2PO_4^+]$	$[CaGlu^+]$	$[Ca^{2+}]$	$[H_3PO_4]$	$[H_2PO_4^-]$	$[HPO_4^{2-}]$	[HGlu]	$[Glu^-]$ I	$\gamma^{2\pm}$	$\gamma^{1\pm}$	Q_{CaGlu2}	Q_G/K_G	Q_{CaHPO4}	Q_P/K_P
0.5	5.2	5.93×10^{-4}	8.83×10^{-2}	5.80×10^{-2}	6.76×10^{-4}	7.68×10^{-4}	8.29×10^{-2}	4.02×10^{-3}	1.96×10^{-5}	5.29×10^{-2}	3.64×10^{-3}	1.58×10^{-2}	0.77	0.59	0.30	0.74	2.39×10^{-3}	20.1	1.46×10^{-5}	1.92×10^{2}
1	4.7	6.65×10^{-4}	8.74×10^{-2}	5.81×10^{-2}	2.79×10^{-4}	8.24×10^{-4}	8.22×10^{-2}	4.12×10^{-3}	5.33×10^{-5}	5.55×10^{-2}	1.47×10^{-3}	3.94×10^{-2}	0.75	0.61	0.30	0.74	2.31×10^{-3}	19.3	6.07×10^{-6}	79.0
2	4.5	6.89×10^{-4}	9.31×10^{-2}	6.11×10^{-2}	1.67×10^{-4}	9.82×10^{-4}	8.73×10^{-2}	4.61×10^{-3}	1.14×10^{-4}	5.91×10^{-2}	7.84×10^{-4}	7.54×10^{-2}	0.71	0.60	0.30	0.74	2.30×10^{-3}	19.3	3.61×10^{-6}	47.2
4	4.3	6.51×10^{-4}	8.90×10^{-2}	5.9×10^{-2}	1.02×10^{-4}	9.45×10^{-4}	8.30×10^{-2}	4.62×10^{-3}	1.71×10^{-4}	5.69×10^{-2}	4.82×10^{-4}	1.11×10^{-1}	0.68	0.58	0.30	0.74	2.11×10^{-3}	17.8	2.23×10^{-6}	29.3
5	4.3	6.99×10^{-4}	9.01×10^{-2}	5.94×10^{-2}	9.12×10^{-5}	1.00×10^{-3}	8.42×10^{-2}	4.80×10^{-3}	2.07×10^{-4}	5.58×10^{-2}	4.12×10^{-4}	0.13	0.66	0.57	0.30	0.74	2.07×10^{-3}	17.4	1.98×10^{-6}	25.9
24	4.1	6.33×10^{-4}	9.04×10^{-2}	6.25×10^{-2}	7.75×10^{-5}	1.11×10^{-3}	8.42×10^{-2}	5.03×10^{-3}	2.85×10^{-4}	6.07×10^{-2}	3.31×10^{-4}	0.16	0.62	0.56	0.30	0.74	1.96×10^{-3}	16.4	1.67×10^{-6}	21.7
48	4.1	6.44×10^{-4}	9.33×10^{-2}	6.33×10^{-2}	7.70×10^{-5}	1.18×10^{-3}	8.68×10^{-2}	5.28×10^{-3}	3.11×10^{-4}	6.14×10^{-2}	3.12×10^{-4}	0.17	0.61	0.57	0.30	0.74	2.02×10^{-3}	16.8	1.65×10^{-6}	21.4
72	4.1	5.96×10^{-4}	9.69×10^{-2}	6.67×10^{-2}	8.70×10^{-5}	1.29×10^{-3}	9.01×10^{-2}	5.45×10^{-3}	3.19×10^{-4}	6.47×10^{-2}	3.38×10^{-4}	0.17	0.61	0.57	0.30	0.74	2.04×10^{-3}	16.9	1.84×10^{-6}	23.7
96	4.1	6.37×10^{-4}	9.01×10^{-2}	6.20×10^{-2}	7.35×10^{-5}	1.11×10^{-3}	8.39×10^{-2}	5.06×10^{-3}	2.98×10^{-4}	6.10×10^{-2}	3.12×10^{-4}	0.17	0.62	0.56	0.29	0.74	1.93×10^{-3}	16.1	1.58×10^{-6}	20.6
144	4.1	6.31×10^{-4}	9.46×10^{-2}	6.74×10^{-2}	8.50×10^{-5}	1.27×10^{-3}	8.79×10^{-2}	5.32×10^{-3}	3.23×10^{-4}	6.54×10^{-2}	3.41×10^{-4}	0.17	0.61	0.57	0.30	0.74	2.00×10^{-3}	16.7	1.81×10^{-6}	23.5
168	4.1	6.21×10^{-4}	8.81×10^{-2}	6.44×10^{-2}	7.52×10^{-5}	1.13×10^{-3}	8.19×10^{-2}	4.99×10^{-3}	3.10×10^{-4}	6.26×10^{-2}	3.24×10^{-4}	0.17	0.61	0.56	0.30	0.74	1.87×10^{-3}	15.7	1.61×10^{-6}	21.1

[a] All concentrations in mol L^{-1}. Precipitation started after approximately 100 h. Conditions for saturation were: 1.4 g of Capolac®; total gluconate concentration of 0.87 mol L^{-1}; ratio between gluconate and δ-gluconolactone of 2:1; equilibration for 168 h at 25 °C. Iterative calculations are based on total calcium and phosphorous concentration as determined by ICP and shown in Fig. 4B. Q_{CaGlu2} corresponds to the ionic product defined by $Q = [Ca^{2+}][Glu^-]^2$. Activity based solubility product $K_{G\text{-}sp\text{-}activity} = K_{sp\text{-}CaGlu2} \times \gamma^{2+} \times (\gamma^-)^2$ was calculated from the concentration based solubility product $K_{sp\text{-}CaGlu2} = (7.1 \pm 0.2) \times 10^{-4}$ for ionic strength = 1.0 (Vavrusova, Munk, & Skibsted, 2013). Q_{CaHPO4} corresponds to the ionic product defined by $Q_P = [Ca^{2+}][HPO_4^{2-}]$. Activity based solubility product $K_{P\text{-}sp\text{-}activity} = K_{sp\text{-}CaHPO4} \times \gamma^{2+} \times \gamma^{2-}$ was calculated from the concentration based solubility product $K_{sp\text{-}CaHPO4} = 8.25 \times 10^{-7}$ for ionic strength = 1.0 (McDowell, Brown, & Sutter, 1971).

Table 2
Ion speciation in supersaturated homogeneous solution at 25 °C resulting from dissolution of 1.4 g of Capolac®, 3.2×10^{-1} mol L^{-1} of sodium gluconate and 3.2×10^{-1} mol L^{-1} of δ-gluconolactone in water (100 mL).[a]

Time (h)	pH	aCa^{2+}	$[Ca^{2+}]_T$	[P]	$[CaHPO_4]$	$[CaH_2PO_4^+]$	$[CaGlu^+]$	$[Ca^{2+}]$	$[H_3PO_4]$	$[H_2PO_4^-]$	$[HPO_4^{2-}]$	[HGlu]	$[Glu^-]$	I	$\gamma^{2\pm}$	$\gamma^{1\pm}$	Q_{CaGlu2}	Q_G/K_{G-}	Q_{CaHPO4}	Q_P/K_{P-}
0.5	4.9	1.16×10^{-3}	8.1×10^{-2}	5.5×10^{-2}	3.03×10^{-4}	9.65×10^{-4}	7.45×10^{-2}	5.46×10^{-3}	4.57×10^{-5}	5.20×10^{-2}	1.36×10^{-3}	2.34×10^{-2}	0.54	0.40	0.29	0.73	1.61×10^{-3}	14.8	7.4×10^{-6}	110.0
2	4.2	1.25×10^{-3}	9.0×10^{-2}	6.1×10^{-2}	8.44×10^{-5}	1.44×10^{-3}	8.16×10^{-2}	7.16×10^{-3}	2.78×10^{-4}	5.89×10^{-2}	2.88×10^{-4}	0.11	0.45	0.40	0.29	0.73	1.47×10^{-3}	13.5	2.1×10^{-6}	30.6
6	4.0	1.24×10^{-3}	9.2×10^{-2}	6.2×10^{-2}	6.28×10^{-5}	1.61×10^{-3}	8.25×10^{-2}	7.96×10^{-3}	4.26×10^{-4}	5.96×10^{-2}	1.93×10^{-4}	0.15	0.41	0.38	0.29	0.73	1.35×10^{-3}	12.5	1.1×10^{-6}	16.8
24	3.9	1.66×10^{-3}	9.3×10^{-2}	6.3×10^{-2}	5.21×10^{-5}	1.75×10^{-3}	8.22×10^{-2}	8.57×10^{-3}	6.64×10^{-4}	6.00×10^{-2}	1.48×10^{-4}	0.18	0.38	0.37	0.29	0.73	1.24×10^{-3}	11.4	1.3×10^{-6}	18.8
48	3.9	1.22×10^{-3}	9.9×10^{-2}	6.7×10^{-2}	5.51×10^{-5}	2.07×10^{-3}	8.72×10^{-2}	9.52×10^{-3}	6.70×10^{-4}	6.38×10^{-2}	1.41×10^{-4}	0.19	0.36	0.38	0.29	0.73	1.26×10^{-3}	11.5	1.3×10^{-6}	19.8
120	3.9	1.09×10^{-3}	9.9×10^{-2}	6.9×10^{-2}	5.72×10^{-5}	2.13×10^{-3}	8.70×10^{-2}	9.49×10^{-3}	6.91×10^{-4}	6.59×10^{-2}	1.47×10^{-4}	0.19	0.36	0.38	0.29	0.73	1.25×10^{-3}	11.5	1.4×10^{-6}	20.5
144	3.8	1.22×10^{-3}	9.9×10^{-2}	6.0×10^{-2}	4.57×10^{-5}	1.83×10^{-3}	8.71×10^{-2}	9.68×10^{-3}	6.19×10^{-4}	5.57×10^{-2}	1.15×10^{-4}	0.20	0.36	0.36	0.29	0.73	1.24×10^{-3}	11.4	2.1×10^{-6}	31.8
192	3.8	1.26×10^{-3}	10.3×10^{-2}	7.0×10^{-2}	6.18×10^{-5}	2.29×10^{-3}	9.11×10^{-2}	1.00×10^{-2}	7.03×10^{-4}	6.72×10^{-2}	1.50×10^{-4}	0.19	0.36	0.38	0.29	0.73	1.30×10^{-3}	11.9	1.5×10^{-6}	22.1

[a] All concentrations in mol L^{-1}. Solution remained homogeneous. Conditions for saturation were: 1.4 g of Capolac®; total gluconate concentration of 0.64 mol L^{-1}; ratio between gluconate and δ-gluconolactone of 1:1; equilibration for 192 h at 25 °C. Iterative calculations are based on total calcium and phosphorous concentration as determined by ICP and shown in Fig. 4B. Q_{CaGlu2} corresponds to the ionic product define by $Q_G = [Ca^{2+}][Glu^-]^2$. Activity based solubility product $K_{G\text{-}sp\text{-}activity} = K_{sp\text{-}CaGlu2} \times \gamma^{2+} \times (\gamma^-)^2$ was calculated from the concentration based solubility product $K_{sp\text{-}CaGlu2} = (7.1 \pm 0.2) \times 10^{-4}$ for ionic strength = 1.0 (Vavrusova et al., 2013). Q_{CaHPO4} corresponds to the ionic product defined by $Q_P = [Ca^{2+}][HPO_4^{2-}]$. Activity based solubility product $K_{P\text{-}sp\text{-}activity} = K_{sp\text{-}CaHPO4} \times \gamma^{2+} \times \gamma^{2-}$ was calculated from the concentration based solubility product $K_{sp\text{-}CaHPO4} = 8.25 \times 10^{-7}$ for ionic strength = 1.0 (McDowell, Brown, & Sutter, 1971).

Table 3
Ion speciation in supersaturated homogeneous solution at 25 °C resulting from dissolution of 1.4 g of Capolac®, 1.7×10^{-1} mol L^{-1} of sodium gluconate and 3.3×10^{-1} mol L^{-1} of δ-gluconolactone in water (100 mL).[a]

Time (h)	pH	aCa^{2+}	$[Ca^{2+}]_T$	[P]	$[CaHPO_4]$	$[CaH_2PO_4^+]$	$[CaGlu^+]$	$[Ca^{2+}]$	$[H_3PO_4]$	$[H_2PO_4^-]$	$[HPO_4^{2-}]$	[HGlu]	$[Glu^-]$	I	$\gamma^{2\pm}$	$\gamma^{1\pm}$	Q_{CaGlu2}	Q_G/K_{G-}	Q_{CaHPO4}	Q_P/K_{P-}
0.5	4.8	1.94×10^{-3}	7.38×10^{-2}	4.77×10^{-2}	5.51×10^{-4}	9.28×10^{-4}	6.62×10^{-2}	6.17×10^{-3}	1.89×10^{-5}	4.41×10^{-2}	2.17×10^{-3}	8.43×10^{-3}	0.45	0.30	0.29	0.73	1.12×10^{-3}	10.3	1.34×10^{-5}	198
1	4.4	2.44×10^{-3}	9.49×10^{-2}	6.20×10^{-2}	3.93×10^{-4}	1.68×10^{-3}	8.43×10^{-2}	8.47×10^{-3}	6.43×10^{-5}	5.84×10^{-2}	1.13×10^{-3}	2.02×10^{-2}	0.40	0.34	0.29	0.73	1.33×10^{-3}	12.2	9.61×10^{-6}	142
2	4.0	2.28×10^{-3}	9.43×10^{-2}	6.19×10^{-2}	2.05×10^{-4}	1.77×10^{-3}	8.35×10^{-2}	8.79×10^{-3}	1.32×10^{-4}	5.93×10^{-2}	5.69×10^{-4}	3.90×10^{-2}	0.38	0.33	0.29	0.73	1.25×10^{-3}	11.5	5.00×10^{-6}	74.1
4	3.8	2.28×10^{-3}	9.40×10^{-2}	6.13×10^{-2}	1.44×10^{-4}	1.83×10^{-3}	8.28×10^{-2}	9.19×10^{-3}	1.98×10^{-4}	5.88×10^{-2}	3.88×10^{-4}	5.47×10^{-2}	0.36	0.36	0.29	0.73	1.19×10^{-3}	11.0	3.56×10^{-6}	53.2
6	3.7	2.10×10^{-3}	9.91×10^{-2}	6.05×10^{-2}	1.15×10^{-4}	1.80×10^{-3}	8.05×10^{-2}	9.08×10^{-3}	2.40×10^{-4}	5.81×10^{-2}	3.00×10^{-4}	6.74×10^{-2}	0.35	0.31	0.29	0.73	1.13×10^{-3}	10.4	2.72×10^{-6}	40.3
24	3.7	2.71×10^{-3}	9.10×10^{-2}	5.9×10^{-2}	8.64×10^{-5}	1.82×10^{-3}	7.96×10^{-2}	9.41×10^{-3}	3.09×10^{-4}	5.70×10^{-2}	2.25×10^{-4}	8.45×10^{-2}	0.34	0.30	0.29	0.73	1.06×10^{-3}	9.8	2.11×10^{-6}	31.3
48	3.6	2.09×10^{-3}	9.79×10^{-2}	6.37×10^{-2}	9.47×10^{-5}	2.15×10^{-3}	8.52×10^{-2}	1.04×10^{-2}	3.62×10^{-4}	6.09×10^{-2}	2.33×10^{-4}	8.65×10^{-2}	0.36	0.31	0.29	0.73	1.11×10^{-3}	10.2	2.32×10^{-6}	34.3
120	3.6	1.77×10^{-3}	9.94×10^{-2}	6.72×10^{-2}	1.04×10^{-4}	2.30×10^{-3}	8.65×10^{-2}	1.05×10^{-2}	3.66×10^{-4}	6.42×10^{-2}	2.41×10^{-4}	8.67×10^{-2}	0.33	0.31	0.29	0.73	1.12×10^{-3}	10.4	2.54×10^{-6}	37.7
144	3.6	2.06×10^{-3}	9.96×10^{-2}	6.67×10^{-2}	1.03×10^{-4}	2.28×10^{-3}	8.67×10^{-3}	1.05×10^{-2}	3.62×10^{-4}	6.37×10^{-2}	2.40×10^{-4}	8.65×10^{-2}	0.33	0.31	0.29	0.73	1.13×10^{-3}	10.4	2.51×10^{-6}	37.1
168	3.6	1.68×10^{-3}	9.95×10^{-2}	6.64×10^{-2}	1.02×10^{-4}	2.27×10^{-3}	8.66×10^{-3}	1.05×10^{-2}	3.61×10^{-4}	6.34×10^{-2}	2.38×10^{-4}	8.65×10^{-2}	0.33	0.31	0.29	0.73	1.12×10^{-3}	10.4	2.51×10^{-6}	37.1

[a] All concentrations in mol L^{-1}. Solution remained homogeneous. Conditions for saturation were: 1.4 g of Capolac®; total gluconate concentration of 0.50 mol L^{-1}; ratio between gluconate and δ-gluconolactone of 1:2; equilibration for 168 h at 25 °C. Iterative calculations are based on total calcium and phosphorous concentration as determined by ICP and shown in Fig. 4B. Q_{CaGlu2} corresponds to the ionic product define by $Q_G = [Ca^{2+}][Glu^-]^2$. Activity based solubility product $K_{G\text{-}sp\text{-}activity} = K_{sp\text{-}CaGlu2} \times \mu^{2+} \times (\gamma^-)^2$ was calculated from the concentration based solubility product $K_{sp\text{-}CaGlu2} = (7.1 \pm 0.2) \times 10^{-4}$for ionic strength = 1.0 (Vavrusova et al., 2013). Q_{CaHPO4} corresponds to the ionic product define by $Q_P = [Ca^{2+}][HPO_4^{2-}]$. Activity based solubility product $K_{P\text{-}sp\text{-}activity} = K_{sp\text{-}CaHPO4} \times \gamma^{2+} \times \gamma^{2-}$ was calculated from the concentration based solubility product $K_{sp\text{-}CaHPO4} = 8.25 \times 10^{-7}$ for ionic strength = 1.0 (McDowell, Brown, & Sutter, 1971).

showed an effect on the pH of the supersaturated solutions (Fig. 6). Different initial and final pH values were observed in the samples containing different combinations of gluconate and gluconolactone. The decrease in pH during incubation is explained by the slow hydrolysis of gluconolactone into gluconic acid. The ratio between gluconate and gluconolactone seems to be important not only for the initiation of the precipitation in the supersaturated systems containing Capolac® but also for increasing the concentration of free calcium in the supersaturated solutions. For increasing concentrations of gluconolactone relative to gluconate, the increase in the concentration of free calcium found by the iterative calculation of the ion speciation further demonstrated the importance of the decreasing pH. A similar effect on free calcium by decreasing pH has been noted for serum calcium in skim milk (Koutina, Knudsen, Andersen, & Skibsted, 2014). Solutions of calcium gluconate with a pH lower than 4 take a long time to crystallise. However, it is important to note that the initial and spontaneous supersaturation occurs at pH higher or equal to 4.8. In these systems, the precipitation is a process of crystallisation without seeding and occurs as a spontaneous process when the system reaches the "labile" region of the solubility curve that describes the supersaturation, as originally suggested by Ostwald in the classical paper from 1897 (Ostwald, 1897), as discussed by Threlfall (2003). For the calcium gluconate supersaturated systems, the transition period from a metastable to a labile state was accordingly found to be very long.

The ratio between the ionic products (Q) and the solubility products (K_{sp}) was calculated to indicate whether the solutions were supersaturated with calcium gluconate or supersaturated with calcium hydrogen phosphate or supersaturated with both:

$$Q_G = [Ca^{2+}] \times [Glu^{-}]^2 > K_{sp}\,(CaGlu_2)$$

$$Q_P = [Ca^{2+}] \times [HPO_4{}^{2-}] > K_{sp}\,(CaHPO_4)$$

The ratio Q/K_{sp} of the solutions containing Capolac® and the three different combinations of gluconate/gluconolactone

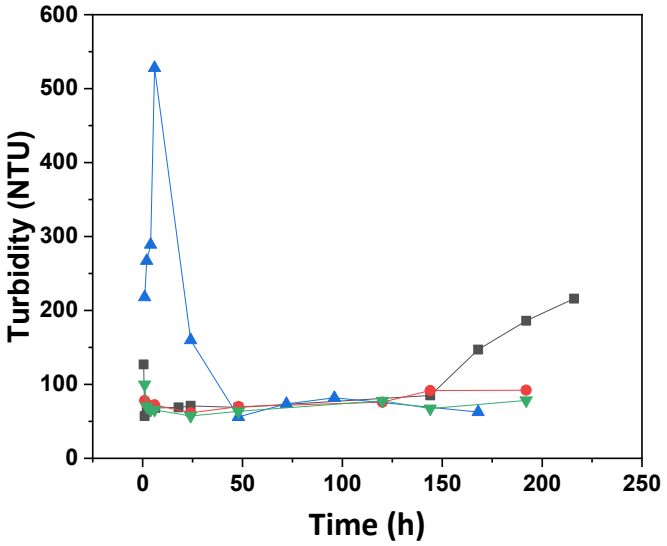

Fig. 6. Turbidity of aqueous solutions containing 1.4 g Capolac® in 100 mL of water and gluconate/gluconolactone with a ratio of 2:1 = 5.8×10^{-2} mol/2.9×10^{-2} mol (■), gluconate/gluconolactone 1:1–3.2×10^{-2} mol/3.2×10^{-2} mol (●), gluconate/gluconolactone 1:1 = 3.2×10^{-2} mol/3.2×10^{-2} mol plus 1×10^{-3} mol of calcium saccharate (▲); gluconate/gluconolactone 1:2 = 1.7×10^{-2} mol/3.4×10^{-2} mol (▼). Turbidity was measured after 30 min and during 8 days of incubation at 25 °C. (For interpretation of the references to color in this figure legend, the reader is referred to the Web version of this article.)

(Tables 1–3) are, during incubation, larger than unity, indicating that the three systems are supersaturated both in relation to $CaGlu_2$ and to $CaHPO_4$. The ratios Q/K_{sp} for $CaGlu_2$ and $CaHPO_4$ decrease during the equilibration period for all the three combinations investigated. However, calcium gluconate was found to precipitate in the solution of the high gluconate experiment (Table 1) in agreement with the increasing supersaturation factor Q/K_{sp} for calcium gluconate, as also observed in the previous study with calcium hydrogen phosphate (Cheng & Skibsted, 2018). The solutions with higher concentrations of gluconolactone relative to gluconate showed no precipitation for the same period of incubation. The supersaturation factor was, for all three set of conditions investigated, larger for $CaHPO_4$ than for $CaGlu_2$ throughout the incubation period; still, $CaHPO_4.2H_2O$ did not precipitate. A comparison between the three conditions shows than $Q/K_{sp} < 12$ apparently is a critical ratio for robustness for precipitation of calcium gluconate. Gluconate ions may, like other anions, by some unknown mechanism inhibit the precipitation of calcium hydrogen phosphate (Holt, Lenton, Nylander, Sørensen, & Teixeira, 2014). The ionic product seems to control the robustness of the supersaturation, while the hydrolysis of gluconolactone seems to control the dynamics of the system including an initial decrease in Q/K_{sp} followed by slower subsequent increase. The equilibrium solubility of the whey minerals depends on the final pH, in contrast to the degree of supersaturation of both calcium gluconate and calcium phosphate as evident from a comparison between Tables 1–3.

For the gluconate/gluconolactone combinations without precipitation for up to one week (ratios 1:1 and 1:2), series of dissolution experiments were performed to determine the critical mass of gluconate necessary to dissolve the calcium salts contained in Capolac®. Suspensions were visually inspected for 6 h under magnetic stirring at 25 °C to investigate which combinations yielded homogeneous supersaturated solutions. The amount of dissolved calcium in Capolac® for the critical combinations of Capolac® and total gluconate for which the solution just became clear, was found to depend linearly on the gluconate concentration for both the ratios gluconate/gluconolactone 1:2 and 1:1, as shown in Figs. 7 and 8, respectively. This linear dependence on the concentration of gluconate for critical combinations of supersaturated solutions was also previously demonstrated for dissolution of $CaHPO_4.2H_2O$ (Cheng & Skibsted, 2018). The linear dependence for the dissolution of Capolac® and $CaHPO_4$ on gluconate concentration are compared in Fig. 9. From linear regression of Fig. 9, the following relationships were obtained:

(i) $[Ca^{2+}] = (0.274 \pm 0.007)\,[\text{Gluconate}] + 0.001$ for a gluconate/gluconolactone ratio of 1:1 for Capolac®
(ii) $[Ca^{2+}] = (0.194 \pm 0.031)\,[\text{Gluconate}] + 0.002$ for a gluconate/gluconolactone ratio of 1:1 for $CaHPO_4.2H_2O$
(iii) $[Ca^{2+}] = (0.545 \pm 0.052)\,[\text{Gluconate}] + 0.002$ for a gluconate/gluconolactone ratio of 1:2 for Capolac®
(iv) $[Ca^{2+}] = (0.375 \pm 0.001)\,[\text{Gluconate}] + 0.005$ for a gluconate/gluconolactone ratio of 1:2 for $CaHPO_4.2H_2O$

A comparison of the critical supersaturation for a gluconate/gluconolactone ratio of both 1:1 and 1:2, shows that for Capolac® and for $CaHPO_4.2H_2O$, a change in pH from 3.8 to 3.6, corresponding to an increase in $[H^+]$ by a factor of 1.6, increases the proportionality for dependence on gluconate concentration by a factor of 2.1 for Capolac® and a factor of 1.9 for $CaHPO_4.2H_2O$, in fair agreement with a proton assisted dissolution according to equation (7). The proportionality factor for dependence of critical supersaturation on gluconate concentration is larger for Capolac® compared with $CaHPO_4.2H_2O$ by a factor of 1.4 at pH = 3.8 and by a factor of 1.5 at pH = 3.6, indicating that other components in Capolac® increases

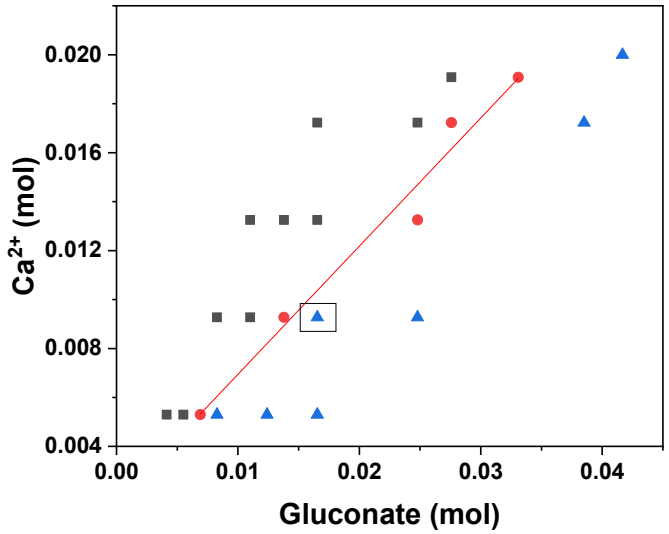

Fig. 7. Critical combination of Capolac® and gluconate for formation of supersaturated solutions in water at 25 °C for a gluconate/gluconolactone ratio of 1:2 as found by visual inspection. Two phase systems are represented by ■; critical calcium/gluconate combinations for formation of homogeneous supersaturated solutions are indicated by ●; ▲ indicate the systems for which homogeneous supersaturated solutions were formed. The critical concentration of total gluconate for a complete dissolution of Capolac® by gluconate, was determined to be $[Ca^{2+}] = (0.545 \pm 0.052)$ [Gluconate] + 0.002. The solution identified with an open square was further analysed for 8 days; see Table 3. (For interpretation of the references to color in this figure legend, the reader is referred to the Web version of this article.)

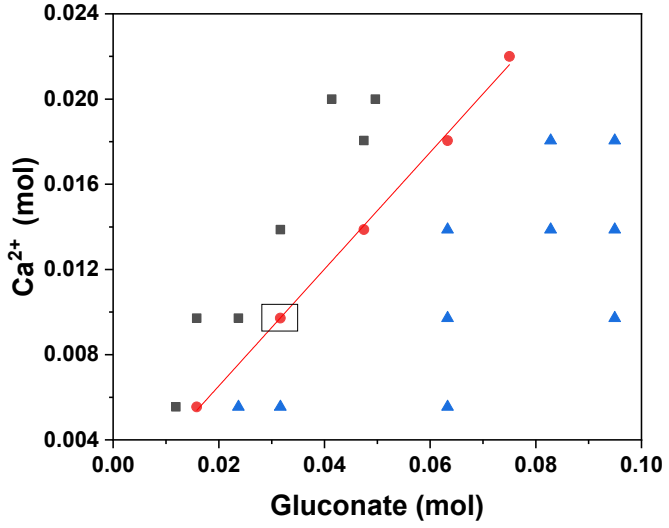

Fig. 8. Critical combination of Capolac® and gluconate for the formation of supersaturated solutions in water at 25 °C for a gluconate/gluconolactone ratio of 1:1 as found by visual inspection. Two phase systems are represented by ■; critical calcium/gluconate combinations for formation of homogeneous supersaturated solutions are indicated by ●; ▲ indicate the systems for which homogeneous supersaturated solutions were formed. The critical concentration of gluconate to a complete dissolution of Capolac® by gluconate, was determined to be $[Ca^{2+}] = (0.274 \pm 0.007)$ [Gluconate] + 0.001 by linear regression. The solution identified with an open square was further analysed for 8 days; Table 2. (For interpretation of the references to color in this figure legend, the reader is referred to the Web version of this article.)

the tendency of supersaturation compared with $CaHPO_4.2H_2O$, but independent of pH. In conclusion, gluconolactone increases the calcium available for dissolution in Capolac®, while gluconate become responsible for the degree of supersaturation.

Notably, the gluconate concentration required to dissolve the same concentration of calcium was found to be lower for Capolac®

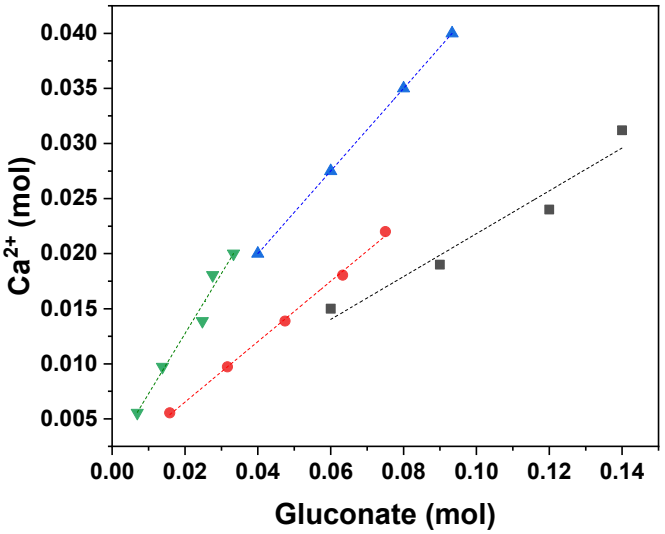

Fig. 9. Critical combinations of $CaHPO_4.2H_2O$ or Capolac®, and gluconate for the formation of homogeneous supersaturated solutions in water at 25 °C for gluconate/gluconolactone with a ratio of 1:1 (■, $CaHPO_4.2H_2O$; ●, Capolac® as a source of calcium) and 1:2 (▲, $CaHPO_4.2H_2O$; ▼, Capolac® as a source of calcium). Data for $CaHPO_4.2H_2O$ are from Cheng and Skibsted (2018). (For interpretation of the references to color in this figure legend, the reader is referred to the Web version of this article.)

compared with $CaHPO_4.2H_2O$ for both ratios gluconate/gluconolactone of 1:1 and 1:2. Capolac® contains other compounds of relevance for improving calcium solubility, such as lactose and hydroxycarboxylates such as citrate. Lactose is one example of calcium-binding compound (Bugg, 1973; Wasserman, 1964). Calcium binding to lactose has been demonstrated in the solid state, but is very weak in aqueous solution. Citrate, especially, has been shown to spontaneously yield strongly supersaturated homogeneous solutions of calcium hydroxycarboxylates (Garcia et al., 2018; Vavrusova et al., 2018, 2017; Vavrusova & Skibsted, 2016). Although the effect of combination of gluconate and citrate for supersaturation of calcium phosphates has not been further explored, sodium citrate has been shown to yield strongly supersaturated solutions when added to calcium gluconate.

Calcium saccharate was previously shown to affect the dynamics of calcium supersaturation. In a previous study (Garcia, Vavrusova, & Skibsted, 2016), calcium saccharate was demonstrated to produce supersaturated solutions of calcium gluconate with a long lag phase for the initiation of precipitation. Calcium saccharate has an increased solubility in the presence of gluconate due to the formation of the complex $CaGlu^+$ in a slow ligand exchange process:

$$CaSac_{(aq)} + Glu^- \rightleftharpoons CaGlu^+ + Sac^{2-} \quad (12)$$

The calcium saccharate complex is thermodynamically favoured over the calcium gluconate complex. However, formation of $CaGlu^+$ is endothermic while formation of CaSac is exothermic, and the ligand exchange seems to become slow with a large activation barrier for formation of $CaGlu^+$ for initiation of precipitation of $CaGlu_2$ in the supersaturated solution (Garcia et al., 2016). Such a large barrier may explain the extremely long lag phase for initiation of precipitation of calcium gluconate in the presence of calcium saccharate.

The formation of a complex between calcium ions and gluconate anions is confirmed from the decrease in the calcium activity upon the addition of sodium gluconate to a suspension containing Capolac® and calcium saccharate (Fig. 4A) together with the increase in the total calcium solubility as evidenced by the increase in

total calcium concentration (Fig. 4B), as also observed in previous studies (Garcia et al., 2016). Homogeneous strongly supersaturated solutions formed upon addition of gluconate/gluconolactone to aqueous Capolac® and calcium saccharate remained supersaturated up to 3 months as saccharate assists the continuous dissolution and formation of $CaGlu^{+}$ in a slow process. The dynamics of this process, however, needs to be further explored for a better mechanistic understanding.

Calcium saccharate has been recognised for stabilising soy milk products fortified with calcium gluconate by preventing precipitation of calcium gluconate (Rasyid & Hansen, 1991). Gluconate alone has now been demonstrated to dissolve whey minerals overshooting the equilibrium solubility of the calcium phosphates presented in a dried whey mineral product. From Fig. 9, the amount of calcium solubilised may be calculated for different concentration of gluconate. For a solution with 0.25 mol L^{-1} gluconate with pH 3.8, approximately 3 g L^{-1} calcium will be present as a robust supersaturation in comparison with around 1.4 g L^{-1} of calcium in acid whey, 40 mg L^{-1} of calcium in a saturated solution of calcium gluconate and 14 mg L^{-1} in a saturated solution of calcium hydrogen phosphate (McDowell, Brown, & Sutter, 1971; Tanguy et al., 2019). Addition of solid calcium saccharate corresponding to 1×10^{-2} mol L^{-1} will ensure a lag phase for precipitation of calcium gluconate and calcium phosphates for more than 3 months. These findings should be further explored in relation to the formulation of functional food for prevention of osteoporosis based on milk minerals.

Acknowledgements

The Danish Dairy Research Foundation and Arla Foods Ingredients Group P/S are thanked for supporting the project. Dr. Daniel Rodrigues Cardoso is thanked for providing the X-ray diffractograms supported by The São Paulo Research Foundation FAPESP - Brazil (Grant 2017/01189-0).

References

Bronner, F. (2009). Recent developments in intestinal calcium absorption. *Nutrition Reviews, 67*, 109–113.
Bugg, C. E. (1973). Calcium binding to carbohydrates. Crystal structure of a hydrated calcium bromide complex of lactose. *Journal of the American Chemical Society, 95*, 908–913.
Cheng, H., & Skibsted, L. H. (2018). Dissolution of calcium hydrogen phosphate in aqueous δ-gluconolactone; long-lasting supersaturation increasing calcium availability. *International Dairy Journal, 84*, 62–71.
Garcia, A. C., Vavrusova, M., & Skibsted, L. H. (2016). Calcium d-saccharate: Aqueous solubility, complex formation, and stabilization of supersaturation. *Journal of Agricultural and Food Chemistry, 64*, 2352–2360.
Garcia, A. C., Vavrusova, M., & Skibsted, L. H. (2018). Supersaturation of calcium citrate as a mechanism behind enhanced availability of calcium phosphates by presence of citrate. *Food Research International, 107*, 195–205.
Gaucheron, F. (2005). The minerals of milk. *Reproduction Nutrition Development, 45*, 473–483.
Gaucheron, F. (2011). Milk and dairy products: A unique micronutrient combination. *Journal of the American College of Nutrition, 30*, 400S–409S.
Harju, M. (2001). Milk sugars and minerals as ingredients. *International Journal of Dairy Technology, 54*, 61–63.
Holt, C., Lenton, S., Nylander, T., Sørensen, E. S., & Teixeira, S. C. M. (2014). Mineralisation of soft and hard tissues and the stability of biofluids. *Journal of Structural Biology, 185*, 383–396.
Kato, K., Toba, Y., Matsuyama, H., Aoki, T., Aoe, S., & Takada, Y. (2002). A novel type of milk calcium has higher calcium bioavailability compared with the hydroxyapatite type of milk calcium. *Journal of Nutritional Science and Vitaminology, 48*, 390–394.
Kelly, P. M., & O'Kennedy, B. T. (2001). The effect of casein/whey protein ratio and minerals on the rheology of fresh cheese gels using a model system. *International Dairy Journal, 11*, 525–532.
Koutina, G., Knudsen, J. C., Andersen, U., & Skibsted, L. H. (2014). Temperature effect on calcium and phosphorus equilibria in relation to gel formation during acidification of skim milk. *International Dairy Journal, 36*, 65–73.
Koutsopoulos, S. (2002). Synthesis and characterization of hydroxyapatite crystals: A review study on the analytical methods. *Journal of Biomedical Materials Research, 62*, 600–612.
Lorieau, L., Le Roux, L., Gaucheron, F., Ligneul, A., Hazart, E., Dupont, D., et al. (2018). Bioaccessibility of four calcium sources in different whey-based dairy matrices assessed by in vitro digestion. *Food Chemistry, 245*, 454–462.
McDowell, H., Brown, W. E., & Sutter, J. R. (1971). Solubility study of calcium hydrogen phosphate. Ion-pair formation. *Inorganic Chemistry, 10*, 1638–1643.
Ostwald, W. (1897). Studien über die Bildung und Umwandlung fester Körper. *Zeitschrift Für Physikalische Chemie, 22*, 289–330.
Pan, H., & Darvell, B. W. (2010). Effect of carbonate on hydroxyapatite solubility. *Crystal Growth and Design, 10*, 845–850.
Prazeres, A. R., Carvalho, F., & Rivas, J. (2012). Cheese whey management: A review. *Journal of Environmental Management, 110*, 48–68.
Rasyid, F., & Hansen, P. M. T. (1991). Stabilization of soy milk fortified with calcium gluconate. *Topics in Catalysis, 4*, 415–422.
Sizo, M. G. (1996). The biotechnological utilization of cheese whey: A review. *Bioresource Technology, 57*, 1–11.
Skibsted, L. H. (2016). Mineral nutrient interaction: Improving bioavailability of calcium and iron. *Food Science and Biotechnology, 25*, 1233–1241.
Skibsted, L. H., & Kilde, G. (1971). Strength and lactone formation of gluconic acid. *Dansk Tidsskrift for Farmaci, 45*, 320–324.
Straub, D. A. (2007). Calcium supplementation in clinical practice: A review of forms, doses, and indications. *Nutrition in Clinical Practice, 22*, 286–296.
Sunyecz, J. A. (2008). The use of calcium and vitamin D in the management of osteoporosis. *Therapeutics and Clinical Risk Management, 4*, 827.
Tanguy, G., Tuler-Perrone, I., Dolivet, A., Santellani, A. C., Leduc, A., Jeantet, R., et al. (2019). Calcium citrate insolubilization drives the fouling of falling film evaporators during the concentration of hydrochloric acid whey. *Food Research International, 116*, 175–183.
Threlfall, T. (2003). Structural and thermodynamic explanations of Ostwald's rule. *Organic Process Research and Development, 7*, 1017–1027.
Vavrusova, M., Danielsen, B. P., Garcia, A. C., & Skibsted, L. H. (2018). Codissolution of calcium hydrogenphosphate and sodium hydrogencitrate in water. Spontaneous supersaturation of calcium citrate increasing calcium bioavailability. *Journal of Food and Drug Analysis, 26*, 330–336.
Vavrusova, M., Garcia, A. C., Danielsen, B. P., & Skibsted, L. H. (2017). Spontaneous supersaturation of calcium citrate from simultaneous isothermal dissolution of sodium citrate and sparingly soluble calcium hydroxycarboxylates in water. *RSC Advances, 7*, 3078–3088.
Vavrusova, M., Munk, M. B., & Skibsted, L. H. (2013). Aqueous solubility of calcium l-lactate, calcium d-gluconate, and calcium d-lactobionate: Importance of complex formation for solubility increase by hydroxycarboxylate mixtures. *Journal of Food and Agricultural Chemistry, 61*, 8207–8214.
Vavrusova, M., & Skibsted, L. H. (2014). Spontaneous supersaturation of calcium d-gluconate during isothermal dissolution of calcium l-lactate in aqueous sodium d-gluconate. *Food and Function, 5*, 85–91.
Vavrusova, M., & Skibsted, L. H. (2016). Aqueous solubility of calcium citrate and interconversion between the tetrahydrate and the hexahydrate as a balance between endothermic dissolution and exothermic complex formation. *International Dairy Journal, 57*, 20–28.
Venkateswarlu, K., Chandra Bose, A., & Rameshbabu, N. (2010). X-ray peak broadening studies of nanocrystalline hydroxyapatite by Williamson–Hall analysis. *Physica B Condensed Matter, 405*, 4256–4261.
Wasserman, R. H. (1964). Lactose-stimulated intestinal absorption of calcium: A theory. *Nature, 201*, 997–999.
Wu, V. M., & Uskoković, V. (2016). Is there a relationship between solubility and resorbability of different calcium phosphate phases in vitro? *Biochimica et Biophysica Acta (BBA) General Subjects, 1860*, 2157–2168.